Biomol NMR Assign (2014) 8:395–404
DOI 10.1007/s12104-013-9526-y

ARTICLE

Yet another polymorph of α-synuclein: solid-state sequential assignments

Julia Gath · Luc Bousset · Birgit Habenstein · Ronald Melki · Beat H. Meier · Anja Böckmann

Received: 4 August 2013 / Accepted: 27 September 2013 / Published online: 10 October 2013

Abstract Parkinson's disease is a neurological human proteinopathy, which is caused by the accumulation of protein aggregates of high molecular mass. α-Synuclein is a major component of these fibrillar, β-sheet rich, insoluble assemblies and is deposited in the form of amyloids. Structural characterization of amyloids is possible by solid-state NMR, although no atomic-resolution structure is available as of today. α-Synuclein, as many other pathology-related fibril-forming proteins, can form a number of different polymorphs that are sometimes tricky to obtain in pure form. Here, we describe the chemical shifts and secondary structure analysis of a polymorph that also adopts mainly β-sheet conformation, with a fibrillar core ranging from residues 38 to 94. In addition, residues 15–20 from the N-terminus found to be part of a rigid ordered β-sheet. The chemical shifts differ substantially from the polymorph we previously assigned.

Keywords α-Synuclein · Fibrils · Solid-state NMR · Assignments · Secondary structure

Biological context

Parkinson's disease is amongst the most frequent and most devastating neurodegenerative diseases. It is tightly associated with the assembly of the protein α-synuclein into high-molecular-weight protein species, which propagate between neurons in the central nervous system. α-Synuclein, which is the principal constituent of the intracellular protein inclusions Lewy bodies that are found in the brain of individuals developing Parkinson's disease, aggregates in vitro into β-sheet rich fibrils. However, numerous polymorphs between different samples, but also within one batch, have been observed.

Recent efforts succeeded in preparing samples with unique polymorphs by careful choice of fibrillization conditions. Two polymorphs (Gath et al. 2012; Comellas et al. 2011) of human α-synuclein and one polymorph of mouse α-synuclein (Lv et al. 2012) could be extensively assigned. The extent of the assignment, the individual chemical shifts and the secondary structure predicted from the chemical shifts differ between the polymorphs, indicating that the three-dimensional (3D) arrangement within the fibrils is substantially different from one form to the other. This shows that sample preparation is a crucial step in fibril structural studies, as structural differences or polymorphs can arise from different production, purification and assembly conditions. Increasing evidence emerges that a variety of forms might have to be considered to establish a structural basis for α-synuclein toxicity. We here describe sequential chemical-shift assignments of an α-synuclein polymorph which has not been described yet, and which

Julia Gath and Luc Bousset have contributed equally to this work.

J. Gath · B. H. Meier (✉)
Physical Chemistry, ETH Zürich, Wolfgang-Pauli-Strasse 10, 8093 Zurich, Switzerland
e-mail: beme@ethz.ch

L. Bousset · R. Melki (✉)
Laboratoire d'Enzymologie et Biochimie Structurales, UPR 3082, CNRS, Avenue de la Terrasse, 91198 Gif-sur-Yvette, France
e-mail: melki@lebs.cnrs-gif.fr

B. Habenstein · A. Böckmann (✉)
Institut de Biologie et Chimie des Protéines, UMR 5086, CNRS/Université de Lyon 1, 7 passage du Vercors, 69367 Lyon, France
e-mail: a.bockmann@ibcp.fr

Table 1 Experimental conditions for fibrillization used in this work, those from previous work Gath et al. (2012), and work described in Comellas et al. (2011) and Heise et al. (2005)

	Buffer	Salts	Protein concentration	Shaking (rpm)	T (°C)	Duration
This work	50 mM Tris–HCl, pH 7.5	150 mM KCl	300 μM	600	37	4 days
Gath et al. (2012)	5 mM Tris–HCl pH 7.5	–	300 μM	600	37	7 days
Comellas et al. (2011)	50 mM Na phosphate buffer, pH 7.4, 0.10 mM EDTA, 0.02 % NaN_3 (w/v)	–	1 mM	250	37	3 weeks
Heise et al. (2005)	25 mM Tris–HCl, pH 7.5, 0.01 % sodium azide	–	220–350 μM	300	37	3 weeks

shows different secondary chemical shifts compared to other assigned specimen.

Methods and experiments

Protein expression and purification

Full-length α-synuclein was expressed in *E. coli* BL21 DE3 codon + cells (Stratagene). Cells were grown in LB medium to an Abs_{600nm} of 0.8 and sedimented at 3,000*g* for 10 min in 1 l tubes. The pelleted bacteria were washed with 200 ml of M9 salt and spun at 3,000 g for 10 min. The bacterial pellets were resuspended in half the volume where they originally grew of M9 media containing 1.75 g of $^{15}NH_4Cl$, 2.5 g of U–^{13}C glucose, 2 mM MgSO4, 0.1 mM $CaCl_2$, 10 μg thiamine per litre of culture. Cells were grown for 30 min at 37 °C and α-synuclein expression was induced by 0.5 mM IPTG for 3 h. The cells were then harvested by centrifugation (4,000*g*, 10 min), resuspended into lysis buffer (10 mM Tris pH 7.5, 1 mM EDTA, 1 mM PMSF) and lysed by sonication. Cell extracts were clarified by centrifugation at 14,000*g*, 30 min. Purification was performed as previously described (Hansen et al. 2011).

Fibrillation was achieved in buffer A (Tris 50 mM pH 7.5, KCl 150 mM) at 300 μM by shaking 1 ml solution aliquots at 37 °C as described (Cohlberg et al. 2002). Fibrils were spun for 20 min at 50,000 rpm on a TL100 ultracentrifuge (Beckman) using the TLA 100.4 rotor. The pellets were washed through 2 cycles of resuspension and sedimentation with buffer B (5 mM Tris pH 7.5). The pelleted material was used to fill a ZrO_2 3.2 mm rotor (Bruker) using home made filling device (Böckmann et al. 2009) spun at 40,000 rpm for 16 h at 18 °C in an SW60 TI rotor and an optima L90-K ultracentrifuge (Beckman). The fibrillization conditions are compared in Table 1 to other forms of sequentially assigned α-synuclein polymorphs described in the literature.

NMR spectroscopy

All dipolar-based spectra were recorded at 20.0 T static magnetic field on a 3.2 mm loaded loop gap coil Bruker probe and processed using topspin 2.1. A shifted (2.4 or 2.6) cosine squared apodization function and automated baseline correction in the direct dimension were applied. The sample temperature was set to 278 K and the MAS rate to 17 kHz. The INEPT spectrum was measured at 14.1 T static magnetic field and at 13 kHz MAS. Further experimental and processing details are given in Table 2. Before starting the assignment process, reproducibility of the sample preparation was checked with 20 ms DARR finger print spectra. However, all assignment spectra were recorded from a single sample.

Assignment and data deposition

The spectra of this new polymorph of α-synuclein are well resolved with a line width at half height in the order of 0.6 ppm. A two-dimensional (2D) ^{13}C–^{13}C correlation spectrum is shown in Fig. 1. The good signal-to-noise ratio obtained for this sample allowed recording of 3D assignment spectra. A representative plane of these spectra is shown in Fig. 2. In the assignment process, a combination of NCA, NCO, NCACO, CANCO, NCOCA (sequential walk) and DARR, NCACB and CCC (side chain assignments) 3D spectra were used. The assignment strategy followed the general approach described in detail before (Habenstein et al. 2011; Schuetz et al. 2010). With these spectra, 90 % of the all carbon atoms and 96 % of all backbone amides between residues 38 and 94 could be assigned (Fig. 3).

For the stretch ranging from residue 79 to residue 92, a second set of chemical shifts was observed, as well as for Ser47. A similar observation was made in mouse α-synuclein, where a doubling of the resonances were observed for residues Gly84, Ala85, Gly86, Ala89 and Gly93 (Lv et al. 2012). In our case, the chemical shifts between the

Table 2 Experimental details

Experiment	DARR 20 ms	NCA	NCO	NCACB	NCACO	NCOCA	CANCO	CCC	INEPT
Spectrometer	850 MHz	850 MHz	850 MHz	850 MHz	850 MHz	850 MHz	850 MHz	850 MHz	600 MHz
Probe	3.2 mm Bruker LLC	3.2 mm Bruker LLC	3.2 mm Bruker LLC	3.2 mm Bruker LLC	3.2 mm Bruker LLC	3.2 mm Bruker LLC	3.2 mm Bruker LLC	3.2 mm Bruker LLC	3.2 mm Bruker
MAS (kHz)	17	17	17	17	17	17	17	17	13
Measurement Time	24 h	8.5 h	8.5 h	3.5 days	2.5 days	4 days	3 days	4 days	3 h
Number of scans	32	16	16	24	8	16	16	4	32
Interscan delay (s)	3	2.5	2.5	2.4	2.2	2.2	2.8	2.2	2.5
Transfer 1	HC-CP	HN-CP	HN-CP	HN-CP	HN-CP	HN-CP	HC-CP	HC-CP	INEPT
Time (ms)	0.5	0.8	0.8	0.8	0.8	0.8	0.3	0.3	d4 = 1.25
Field (kHz)	63(H)/47(C)	53(H)/39(N)	52(H)/39(N)	53(H)/39(N)	68(H)/50(N)	68(H)/50(N)	68(H)/52(C)	68(H)/52(C)	–
Shape	Tangent(H) D = 13 kHz	Tangent(H) D = 21 kHz	Tangent(H) D = 21 kHz	Tangent(H) D = 21 kHz	Tangent(H) D = 27 kHz	Tangent(H) D = 27 kHz	Tangent(H) D = 14 kHz	Tangent(H) D = 14 kHz	–
Carrier (ppm)	101	120	121	120	120	120	44	44	–
Transfer 2	DARR	NCA-CP	NCO-CP	NCA-CP	NCA-CP	NCO-CP	NCA-CP	DREAM	–
Time (ms)	20	5	5.5	5	5.5	5.5	5.5	4	
Field (kHz)	17(H)	90(H)/20(C)/ 6(N)	100(H)/11(C)/ 6(N)	90(H)/20(C)/ 6(N)	85(H)/10(C)/ 6.5(N)	100(H)/11(C)/ 6(N)	85(H)/10(C)/ 6.5(N)	100(H)/12(C)	
Shape	–	Tangent(C) D = 4 kHz	Tangent(C) D = 2 kHz	Tangent(C) D = 4 kHz	Tangent(C) D = 2 kHz	Tangent(C) D = 2 kHz	Tangent(C) D = 2 kHz	Tangent(C) D = 7 kHz	
Carrier (ppm)	–	59	170	59	58	170	58	54	
Transfer 3	–	–	–	DREAM	DARR/MIRROR	DARR/MIRROR	NCO-CP	DARR/MIRROR	–
Time (ms)				4	20	50	5.5	80	
Field (kHz)				90(H)/14C)	21(H)	21(H)	100(H)/11(C)/ 6(N)	21(H)	
Shape				Tangent(C) D = 8 kHz	–	–	Tangent(C) D = 2 kHz	–	
Carrier (ppm)				51	–	–	170	–	
t1 increments	896	768	768	56	80	72	104	192	128
Sweep width (kHz)	45	30	30	4.7	6.5	6	10	20	12.5
Carrier (ppm)	101	120	121	120	120	120	44	40	4.5
Acq. time (ms)	9.9	12.8	12.8	5.9	6.2	6	5.2	4.8	5.1
td proc	1,024	1,024	1,024	256	256	256	256	512	1,024

Table 2 continued

Experiment	DARR 20 ms	NCA	NCO	NCACB	NCACO	NCOCA	CANCO	CCC	INEPT
Window function	Qsine 2.6	Qsine 2.6	Qsine 2.6	Qsine 2.6	Qsine 2.4	Qsine 2.4	Qsine 2.4	Qsine 2.6	Qsine 2.5
t2 increments	1,536	1,280	1,280	96	144	132	68	192	2,048
Sweep width (kHz)	50	50	50	9.6	12	11	5.25	20	50
Carrier (ppm)	101	100	103	53		173	120	40	100
Acq. time (ms)	15.4	12.8	12.8	5	6	6	6.5	4.8	20.5
td proc	2,048	2,048	2,048	256	512	256	256	512	4,096
Window function	Qsine 2.6	Qsine 2.6	Qsine 2.6	Qsine 2.6	Qsine 2.4	Qsine 2.4	Qsine 2.4	Qsine 2.6	Qsine 3
t3 increments	–	–	–	1,536	2,048	2,048	1,280	2,560	–
Sweep width (kHz)				70	100	100	50	100	
Carrier (ppm)				100	100	100	100	100	
Acq. time (ms)				11.1	10.3	10.3	12.8	12.8	
td proc	–	–	–	2,048	4,096	4,096	4,096	4,096	–
Window function				Qsine 2.6	Qsine 2.6	Qsine 2.6	Qsine 2.6	Qsine 2.4	
Decoupling	SPINAL64	SPINAL64	SPINAL64	SPINAL64	SPINAL64	SPINAL64	SPINAL64	SPINAL64	SPINAL64
Field (kHz)	100	90	100	90	85	85	85	85	100

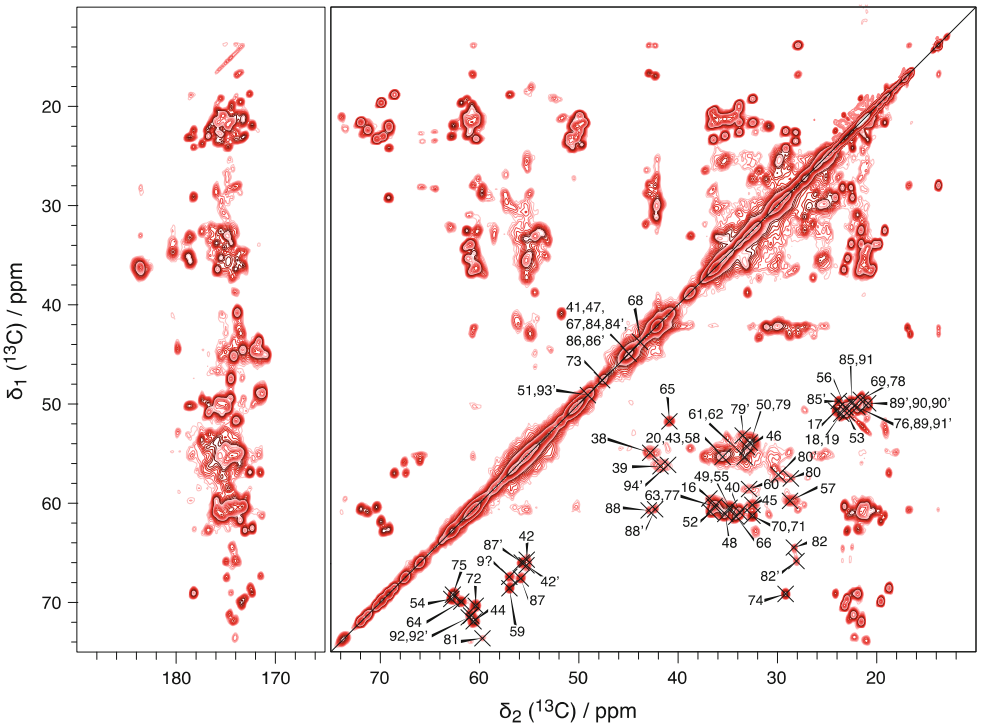

Fig. 1 2D ^{13}C–^{13}C DARR spectrum of α-synuclein fibrils recorded with a mixing time of 20 ms at a magnetic field of 20.0 T. The data was zero-filled and apodized in both dimensions using shifted squared sine-bell function (qsine 2.6). All assigned correlations between Cα and Cβ are labeled with the residue number. *Dashed numbers* refer to the second set of shifts in the doubled stretch

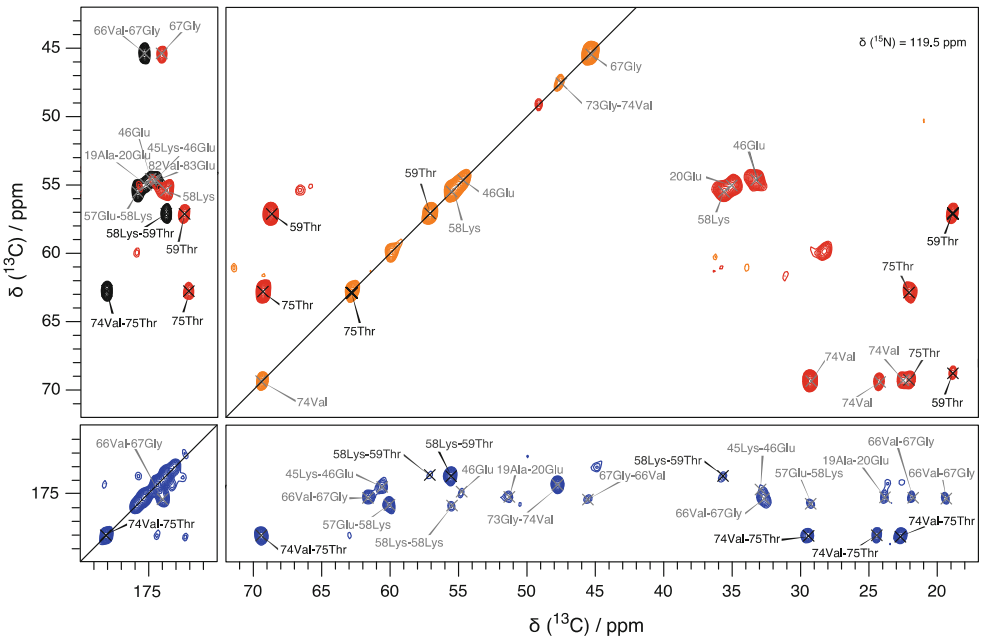

Fig. 2 Planes of 3D CANCO (*black*), NCOCA (*blue*) and NCACB (*red*) spectra recorded at a static magnetic field of 20.0 T. For experimental details see Table 2. The data were analyzed using the CCPN software (Stevens et al. 2011; Vranken et al. 2005). *Grey labels* mean that the maximum of the corresponding peak is at a slightly different ^{15}N chemical shift, therefore leading to weaker signals in the plane presented

two sets of resonances vary the most for amide and Cβ values, which are known to be most sensitive to small changes in the backbone dihedral angles. Figure 4 shows the differences in chemical shift for Cα, Cβ, C and N, as well as a comparison of intensities and line widths of the doubled peaks in the NCACB spectrum. Both sets of peaks have roughly the same intensity. They probably correspond to two α-synuclein monomers in one asymmetric unit of

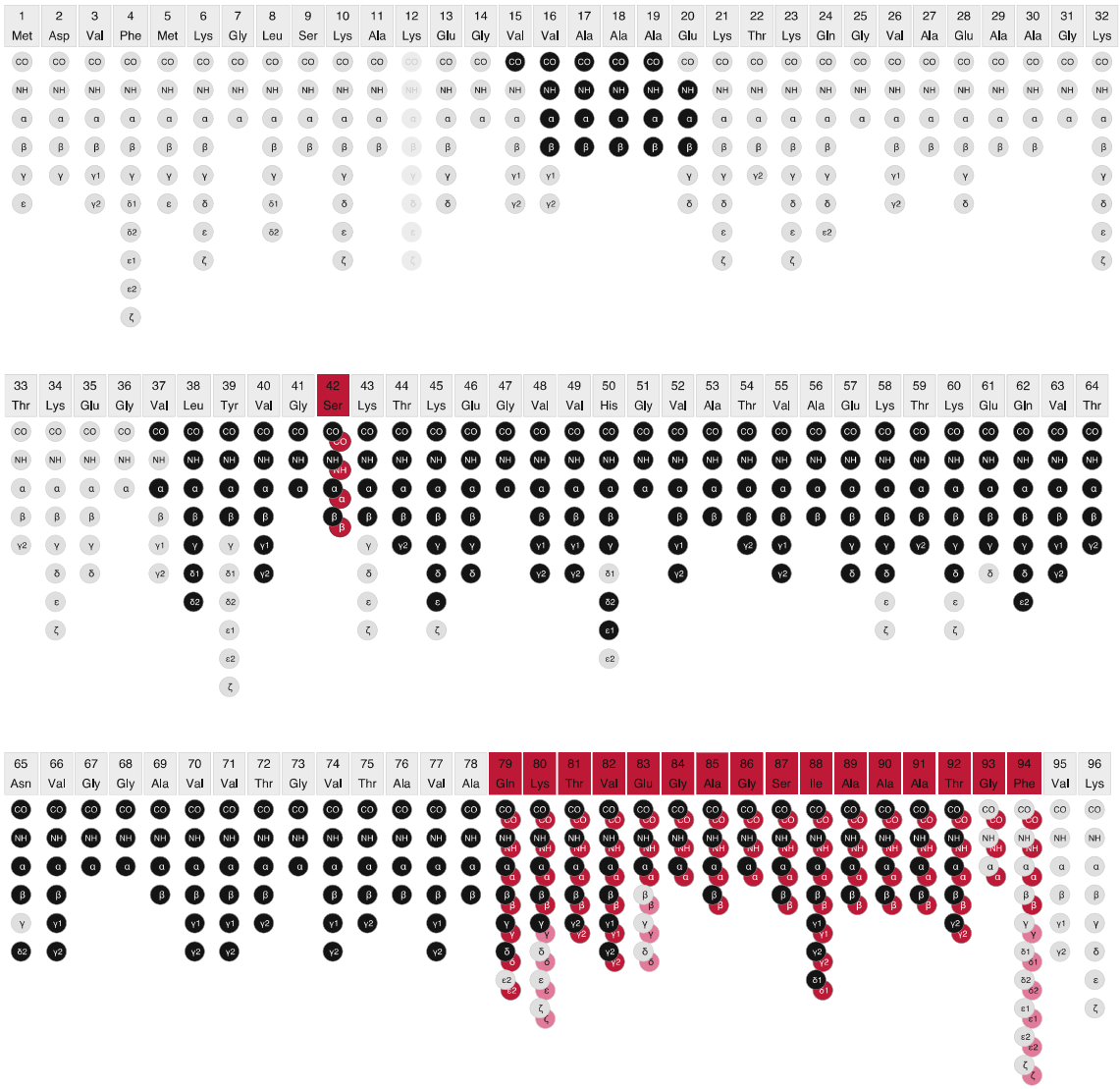

Fig. 3 Assignment graph [created using the CCPN software (Stevens et al. 2011)] of the N-terminal 96 amino acids of α-synuclein. Residues for which two sets of chemical shifts were found are marked in *red*. The *red* assignment graph belongs to chain B. For residues 1–15 and 21–37 only tentative or no assignments could be obtained due to spectral overlap or missing sequential connections. No assignments could be obtained for the flexible parts 95–140

the fibril, as recently found in Ure2p C-terminal (Habenstein et al. 2011). Therefore, a second chain, B, was introduced for these residues. However, the assignment of Ser47 to chain A and B is arbitrary as there is no contact to the C-terminal residues visible in our spectra. The link between residues Glu83 and Gly84 is also ambiguous due to almost identical chemical shifts. The labeling of the chains might be interchanged at this point. The assignment of both chains is deposited in the BMRB under the accession number 18860.

Secondary chemical-shift differences between the Cα and Cβ resonances for both chains are given in Fig. 5. They are mainly negative, showing that this new polymorph, in analogy to the three previously assigned polymorphs, mainly adopts β-sheet conformation. For the two chains distinguished in this polymorph, the secondary shifts differences are very similar. Therefore, the three dimensional structure of the two hypothetic monomers of α-synuclein in the asymmetric unit should be very similar, with slight differences in the C-terminal region.

A careful analysis of the 20 ms DARR, the NCA and the NCACB spectrum showed that some of the resonances are still unexplained. These were combined into 21 spin systems, for some of which the amino-acid type could be identified. However, sequential assignment turned out to be

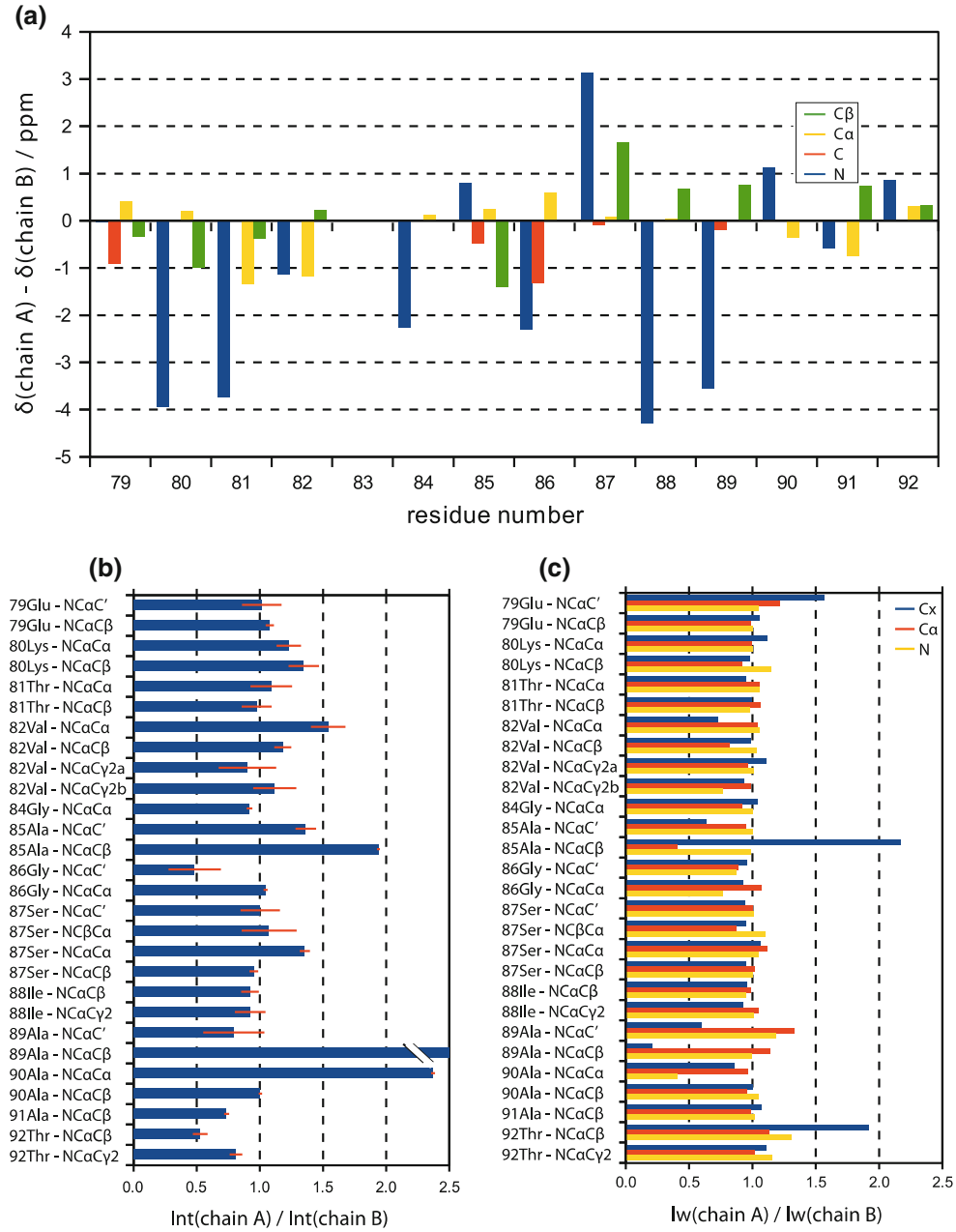

Fig. 4 **a** Differences in the peak positions in the NCACB spectrum for the two sets of peaks (chain A and chain B) for the stretch from residue 79–90. Differences are largest for nitrogen and Cβ shifts. Those two are known to be most sensitive to small changes in the backbone dihedral angles. Glu83 is not visible in the NCACB spectrum. The tolerance for chemical shifts is 0.2 ppm for carbon and 0.4 ppm for nitrogen. Comparison of the two sets of NCACB peaks originating form the doubled stretch in terms of intensity (**b**) and line width (**c**). The relative ratio of intensities is close to one for most of the peaks. These differences could be tracked to problems with signal overlap. *Error bars* correspond to the statistical error calculated from the noise level of the spectrum and do not include systematic errors due to overlapping peaks

impossible, as they either have no sequential contacts or spectral overlap was too severe to allow for a sequential walk. Some spin systems were only visible in 2D spectra. A few spin systems could be tentatively assigned to some of the 32 unassigned residues in the N-terminal region. Indeed, it seems likely that all unexplained resonances stem from the N-terminus. However, it is clear that not all N-terminal residues are visible in the spectra. Figure 6 compares the number of unassigned spin systems with the occurrence of unassigned amino acid types in the N-terminal part. Those tentative assignments are not deposited in the BMRB and not considered in the following.

No indications pointing to the presence of rigid, ordered parts in the C-terminal 46 residues could be observed. This

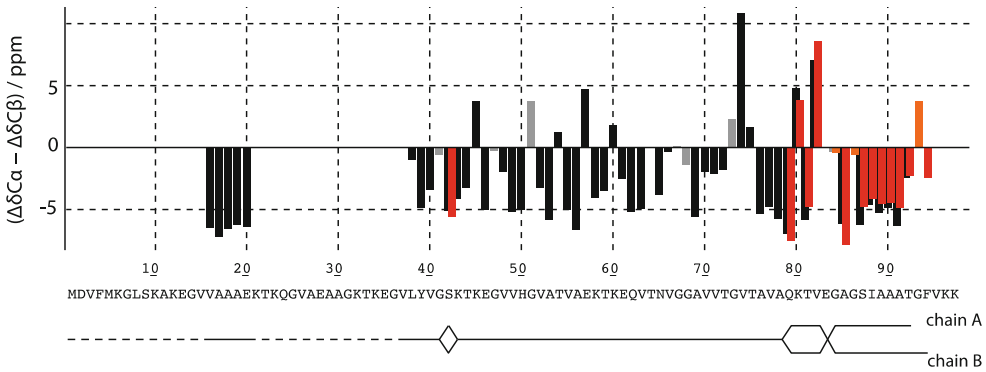

Fig. 5 Differences between secondary chemical shifts of Cα and Cβ resonances relative to their random coil shift tabulated by Wishart and Sykes (1994) of the sequentially assigned residues of α-synuclein. *Red bars* stand for the secondary chemical shifts of the doubled stretch starting at residue 79. For glycine residues only the deviation of the Cα shift from the random coil value is plotted. Glycines are indicated in *grey* and in *orange* for chain A and chain B, respectively. Three *negative bars* in a row are indicative for β-sheet secondary structure. Underneath the Figure the extent of the peak doubling is indicated with the points, where the assignment to chain A and chain B may or may not be interchanged

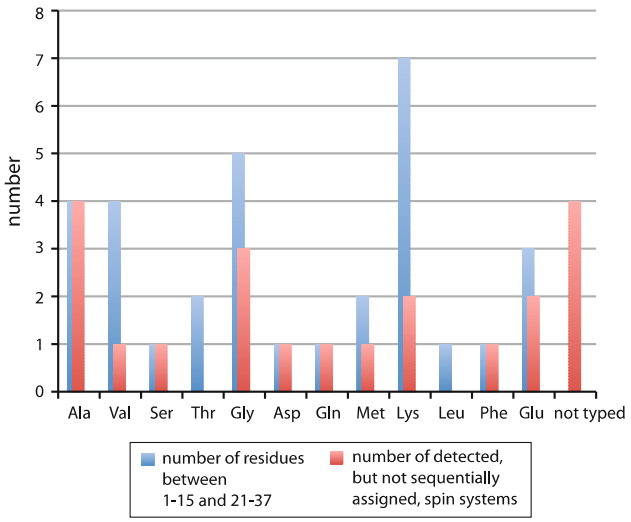

Fig. 6 Comparison between the number of amino-acid residues in the N-terminus, (more specifically the stretches from residue 1–15 and residue 21–37 which are not assigned in this paper) and the number of experimentally detected but not sequentially assigned spin systems

is not surprising as in all forms studied so far, at least the last 40 residues were found to be flexible and unstructured. In Fig. 7 a ^{1}H–^{13}C INEPT spectrum of the α-synuclein fibrils studied is shown. All peaks, besides the threonine resonances (vide infra) could be explained assuming that the 46 residues C-terminal residues, which are not detected in the CP-based experiments, are flexible. For residues preceding a proline, the Hα and Cα shifts differ from the normal random coil values. Therefore, they can be assigned sequence specifically. In the C-terminus of α-synuclein there are five proline residues, and all five preceding residues can be identified in the INEPT spectrum. As there are no threonines present in the C-terminal portion, the threonine resonances come probably from residual monomers in the rotor. For α-synuclein fibrils obtained under similar fibrilization conditions, it was shown, that α-synuclein fibrils are in a temperature-dependent equilibrium with the monomers (Kim et al. 2009). However, they might also be assigned to Thr22 or Thr33, located in the region of the molecule where no CP-based signals could be assigned indicating at least some dynamics for this stretch of amino acids.

In summary, the number and location of residues forming the rigid core region of the new polymorph we report is comparable to the two polymorphs of human α-synuclein described by Comellas et al. (2011) and Heise et al. (2005) and the mouse α-synuclein described by Lv et al. (2012). However, the chemical shifts, and therefore also the secondary chemical-shift differences which are used as a proxy for secondary structure, differ substantially from those two polymorphs (Fig. 8). The new polymorph shares features with a different form of human α-synuclein described by Gath et al. (2012) as at least some resonances from the N-terminal region are observed. Interestingly, while all five polymorphs reported so far have a flexible, unstructured C-terminus in common, they differ by the amino-acid stretches involved in β-sheet rich structures constituting the core of the fibrils. How the differences in structure impact fibrils growth propensity and toxicity will certainly be a central aspect in further investigations.

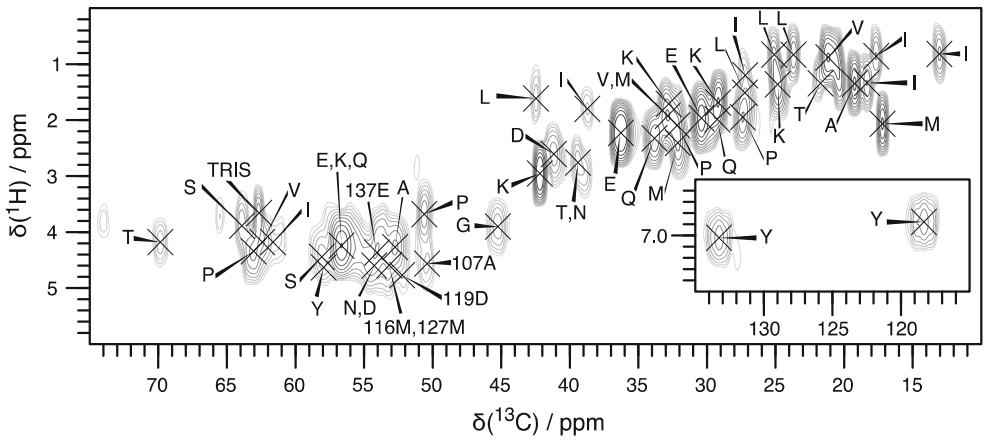

Fig. 7 ^{1}H–^{13}C INEPT spectrum of UL α-synuclein fibrils. The *insert* shows the aromatic region of the spectrum. The amino-acid type specific assignment is given on the spectrum. For residues preceding a proline, the sequential assignment of the Hα–Cα cross peak is possible. All peaks can be explained with the amino acid composition of the 46 C-terminal residues. The Thr Hβ–Cβ cross peak might indicate the presence of an equilibrium between monomers and fibrils in the sample or might come from the unassigned Thr22/Thr33

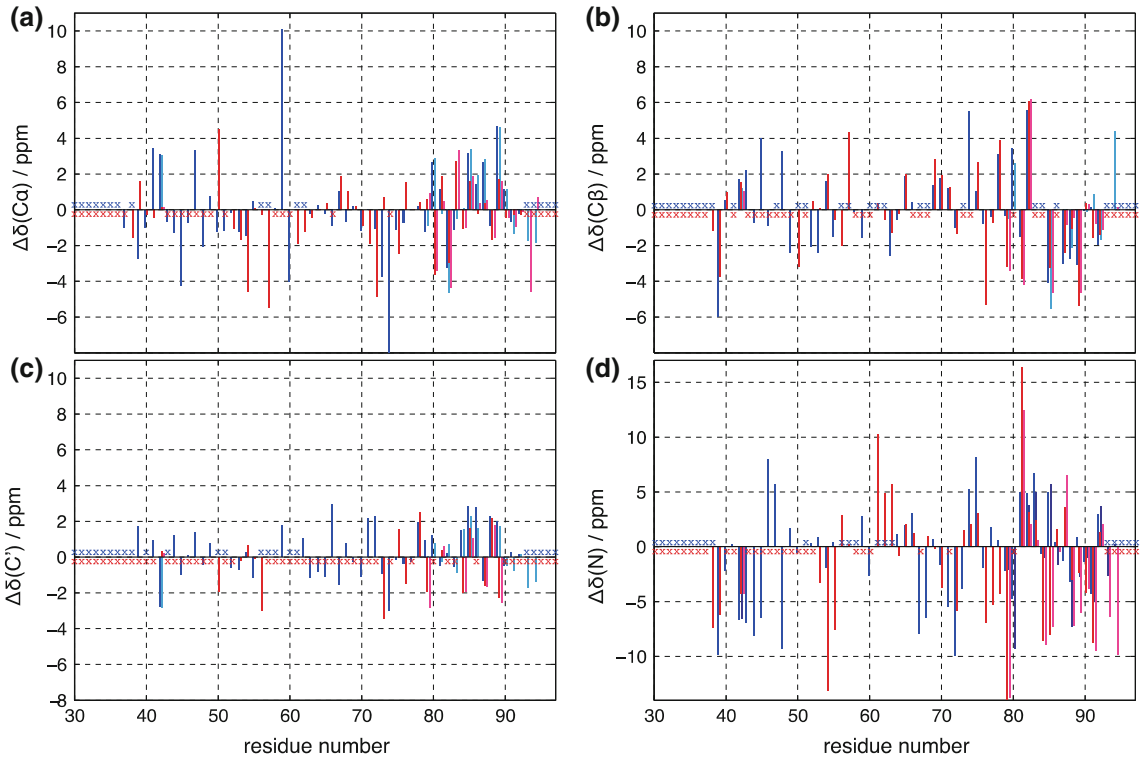

Fig. 8 Deviation of the chemical shifts of the α-synuclein polymorph presented in this assignment note from previously assigned fibril forms for **a** Cα, **b** Cβ, **c** C′ and **d** N. Deviations form the polymorph assigned by Comellas et al. (2011) are shown in *blue* and from the polymorph assigned by Heise et al. (2005) in *red*. Values referring to chain B of our form are indicated with *light blue* and *light red bars*, respectively. Residues, where none or only one assignment is available, so that no difference could be calculated, are marked with *crosses*

Acknowledgments This work was supported by the Agence Nationale de la Recherche (ANR-11-BSV8-021-01), the ETH Zurich, the Swiss National Science Foundation (Grant 200020_124611), the Era-Net Neuron (project MIPROTRAN, ANR-08-NEUR-001-01) and the Centre National de la Recherche Scientifique. We also acknowledge support from the European Commission under the Seventh Framework Programme (FP7), contract Bio-NMR 261863.

References

Böckmann A, Gardiennet C, Verel R, Hunkeler A, Loquet A, Pintacuda G, Emsley L, Meier BH, Lesage A (2009) Characterization of different water pools in solid-state NMR protein samples. J Biomol NMR 45(3):319–327

Cohlberg JA, Li J, Uversky VN, Fink AL (2002) Heparin and other glycosaminoglycans stimulate the formation of amyloid fibrils from α-synuclein in vitro. Biochemistry 41(5):1502–1511

Comellas G, Lemkau LR, Nieuwkoop AJ, Kloepper KD, Ladror DT, Ebisu R, Woods WS, Lipton AS, George JM, Rienstra CM (2011) Structured regions of α-synuclein fibrils include the early-onset Parkinsons disease mutation sites. J Mol Biol 411(4):881–895

Gath J, Habenstein B, Bousset L, Melki R, Meier BH, Böckmann A (2012) Solid-state NMR sequential assignments of α-synuclein. Biomol NMR Assign 6(1):51–55

Habenstein B, Wasmer C, Bousset L, Sourigues Y, Schütz A, Loquet A, Meier BH, Melki R, Böckmann A (2011) Extensive de novo solid-state NMR assignments of the 33 kDa C-terminal domain of the Ure2 prion. J Biomol NMR 51(3):235–243

Hansen C, Angot E, Bergström A-L, Steiner JA, Pieri L, Paul G, Outeiro TF, Melki R, Kallunki P, Fog K, Li J-Y, Brundin P (2011) α-Synuclein propagates from mouse brain to grafted dopaminergic neurons and seeds aggregation in cultured human cells. J Clin Invest 121(2):715–725

Heise H, Hoyer W, Becker S, Andronesi O, Riedel D, Baldus M (2005) Molecular-level secondary structure, polymorphism, and dynamics of full-length α-synuclein fibrils studied by solid-state NMR. Proc Natl Acad Sci USA 102(44):15871–15876

Kim H-Y, Cho M-K, Kumar A, Maier E, Siebenhaar C, Becker S, Fernández CO, Lashuel HA, Benz R, Lange A, Zweckstetter M (2009) Structural properties of pore-forming oligomers of α-synuclein. J Am Chem Soc 131(47):17482–17489

Lv G, Kumar A, Giller K, Orcellet ML, Riedel D, Fernandez CO, Becker S, Lange A (2012) Structural comparison of mouse and human α-synuclein amyloid fibrils by solid-state NMR. J Mol Biol 420(1–2):99–111

Schuetz A, Wasmer C, Habenstein B, Verel R, Greenwald J, Riek R, Böckmann A, Meier BH (2010) Protocols for the sequential solid-state NMR spectroscopic assignment of a uniformly labeled 25 kDa protein: HET-s(1-227). ChemBioChem 11(11):1543–1551

Stevens TJ, Fogh RH, Boucher W, Higman VA, Eisenmenger F, Bardiaux B, van Rossum B-J, Oschkinat H, Laue ED (2011) A software framework for analysing solid-state MAS NMR data. J Biomol NMR 51(4):437–447

Vranken W, Boucher W, Stevens T, Fogh R, Pajon A, Llinas P, Ulrich E, Markley J, Ionides J, Laue E (2005) The CCPN data model for NMR spectroscopy: development of a software pipeline. Proteins 59(4):687–696

Wishart DS, Sykes BD (1994) The 13C Chemical-Shift Index: a simple method for the identification of protein secondary structure using 13C chemical-shift data. J Biomol NMR 4(2):171–180